Research Article BEU Fen Bilimleri Dergisi 15(1): 201-215 (2026) DOI: 10.17798/bitlisfen.1788646

BİTLİS EREN UNIVERSITY
FEN BİLİMLERİ DERGİSİ
ISSN: 2147-3129 / e-ISSN: 2147-3188

MULTI-CRITERIA OPTIMIZATION AND COMPARATIVE EVALUATION OF PASSIVE HARMONIC FILTERS USING ADVANCED META-HEURISTIC ALGORITHMS

Ahmet NUR [1*], Faruk KÜRKER [2]

[1] *Bitlis Eren University, Electrical-Electronics Engineering Department, Bitlis, Türkiye*
[2] *Adıyaman University, Electrical-Electronics Engineering Department, Adıyaman, Türkiye*
**** Corresponding Author:*** *anur@beu.edu.tr*

Article Info

Received: *September 22, 2025*
Revised: *October 21, 2025*
Accepted: *December 9, 2025*

Keywords
Harmonic distortion,
Passive harmonic filter,
Optimization algorithms

ABSTRACT

Harmonics, which negatively affect power quality, are among the primary problems caused by non-linear loads. These harmonics lead to distortions in voltage and current waveforms, excessive current and voltage surges, insulation failures, and malfunctions in power electronics-based equipment in industrial power systems. Therefore, the development of optimization-based harmonic filter design methods suitable for industrial applications is of great importance for improving power quality and ensuring system reliability. In this study, five different passive harmonic filter topologies (Single-Tuned Harmonic Filter, First-Order High-Pass Filter, Second-Order High-Pass Filter, Third-Order High-Pass Filter, and C-Type Filter) were optimized under a multi-criteria framework using four advanced meta-heuristic algorithms (Genetic Algorithm – GA, Particle Swarm Optimization – PSO, Differential Evolution – DE, and Grey Wolf Optimization – GWO). The optimization process simultaneously minimizes three fundamental performance criteria: average total harmonic distortion (THDI_mean), the IEEE-519 standard violation penalty, and reactive power consumption (QC). Results show that Single-Tuned filters optimized with PSO and DE algorithms achieved the lowest harmonic distortion (THDI_mean ≈ 0.577), while C-Type filters stood out with low reactive power requirement (~1.9×10^4 VAr) and superiority in suppressing third harmonics. High-pass filters (1st–3rd order) performed worse across all algorithms. Multi-criteria optimization, simultaneously considering harmonic reduction, compliance with standards, and reactive power balance, offers more balanced and industrially applicable solutions than single-criterion approaches.

1. INTRODUCTION

The rapid advancement of technology has increased load diversity and the use of non-linear equipment in power systems, making power quality problems inevitable in modern energy infrastructure. Power quality is defined, in its simplest terms, as the uninterrupted transmission of energy at a constant frequency and in a sinusoidal waveform. However, non-linear loads disrupt this sinusoidal structure by causing unwanted harmonic components to form in the system. These harmonics are produced by equipment such as rectifiers, inverters, welding machines, arc furnaces, motor drives, uninterruptible power supplies, and frequency converters. The effects of harmonics on power systems are quite serious: they cause circuit breakers to trip unnecessarily, excessive heating in transformers and motors, increased line losses, deterioration of the dielectric properties of capacitors and cables, reduced system efficiency, interference in communication lines, mechanical vibrations, resonance events, and faulty operation of relays. The IEEE defines power quality as 'the provision of suitable energy and grounding conditions for sensitive electronic equipment [1-5]. These effects are not only related to technical limitations; they are also critical for energy efficiency, system safety, and economic sustainability. Therefore, reducing harmonics is a fundamental engineering priority for the safe, economical, and environmentally sustainable operation of energy systems.

Among existing solutions, passive harmonic filters (PHF) remain among the most widely used methods in the industry due to their high robustness, low cost, and simple structure. However, it is known that different PHF topologies (single-tuned, first, second, third-order high-pass, and C-type) exhibit different performance in terms of harmonic suppression, reactive power balance, and cost. Many studies in the literature have only examined a specific filter topology or a limited number of optimisation methods; critical issues such as compliance with the IEEE-519 standard, reactive power limits, and multi-criteria performance evaluation have generally been overlooked [6, 7].

This study proposes a comprehensive multi-criteria optimisation framework that simultaneously optimises five different passive harmonic filter topologies (single-tuned, 1st, 2nd and 3rd order high-pass, and C-type) under four advanced heuristic optimisation algorithms (Genetic Algorithm – GA, Particle Swarm Optimisation – PSO, Difference Evolution – DE, and Grey Wolf Optimisation – GWO) simultaneously. The framework minimises the average total harmonic distortion (THDI_mean), the IEEE-519 violation penalty, and the reactive power consumption (QC ≤ 40 kVAr). The results show that the PSO and DE algorithms yield the lowest THDI_mean value (~0.577), while C-type filters stand out for their low reactive power requirement (~1.9×10^4 VAr) and superior suppression of third harmonics.

Although significant progress has been made in the literature on harmonic reduction, a detailed review of existing studies reveals some fundamental research gaps:

- Most studies evaluate only a single PHF topology and do not provide a comparative analysis of different filter structures under the same conditions.
- Optimisations are generally single-criterion; harmonic distortion (THDI), reactive power balance (QC) and IEEE-519 compliance are not considered together.
- The relative impact of different heuristic algorithms, such as GA, PSO, DE, and GWO, on filter performance has not been systematically investigated.
- The engineering trade-off between harmonic suppression and reactive power limitation (QC ≤ 40 kVAr) has not been quantitatively defined in most studies; this limits industrial applicability and stability.

The primary objective of this study is to develop an integrated, reproducible optimisation approach that simultaneously provides harmonic suppression, compliance with the IEEE-519 standard, and reactive power stability. Inadequate harmonic control in industrial facilities leads to serious consequences, including excessive heating in transformers and motors, false triggering of protection elements, increased line losses, instability in compensation systems, and to penalties for IEEE-519 violations. Therefore, the proposed approach not only contributes academically but also aims to provide a solution that is applicable, balanced, and sustainable on an industrial scale.

Consequently, by presenting a new optimisation approach that comprehensively addresses harmonic suppression, compliance with standards, and reactive power stability, the study contributes to the development of applicable, balanced, and reliable design strategies for industrial systems.

2. HARMONIC FILTER TOPOLOGIES

Passive harmonic filters are widely used in industrial power systems to reduce current and voltage distortions caused by non-linear loads. Filter topologies are classified according to their impedance characteristics and the targeted harmonic orders. The most commonly used passive filter configurations are single-tuned harmonic filters, first-order high-pass filters, second-order high-pass filters, third-order high-pass filters, and C-type filters. Each topology exhibits different impedance behaviors that vary with frequency, offering advantages and limitations in terms of selectivity, reactive power compensation, harmonic suppression, and cost-effectiveness. Table 1 summarizes the commonly used passive harmonic filter configurations, along with their associated harmonic ranges and technical descriptions [8-12].

Table 1. Passive harmonic filter topologies and technical descriptions

Filter	Targeted / Effective Harmonics	Technical Remark
Single-Tuned Harmonic Filter	Specific low-order harmonics (commonly 5th, 7th, 11th, 13th)	Most commonly used; tuned to a specific harmonic order
1st-Order High-Pass Filter	High-order harmonics above tuning frequency	Simple design; mainly used for high-frequency suppression
2nd-Order High-Pass Filter	Low and mid-order harmonics with better selectivity than first-order high-pass filter	Provides better filtering of selected bands than first-order high-pass filter
3rd-Order High-Pass Filter	Wide range of low, mid, and high-order harmonics with sharper attenuation	Improved filtering with higher selectivity; steeper roll-off
C-Type Filter	Low-order harmonics (especially 3rd and below)	Efficient at suppressing 3rd harmonic and reduces fundamental losses

2.1. Single-Tuned Harmonic Filter

Single-tuned harmonic filters are classic RLC shunt circuits that exhibit narrow-band characteristics for suppressing a specific harmonic order. The impedance of these filters in Laplace space is;

$$Z_f(s) = \frac{LCs^2 + Rs + 1}{Cs} \tag{1}$$

Here, $s=\sigma+j\omega$ represents the complex Laplace operator. In single-stage harmonic filters, the resonance frequency is set to match the frequency of the target harmonic component, as shown in the equation (2);

$$f = \frac{1}{2\pi\sqrt{LC}} \tag{2}$$

The quality factor indicating tuning sharpness is [13, 14]:

$$Q = \sqrt{\frac{L}{C}} \cdot \frac{1}{R} \tag{3}$$

A high Q value provides a narrow-band and selective attenuation effect, while a low Q value leads to a wider-band but less selective behavior. Single-tuned harmonic filters are commonly used to suppress the 5th and 7th harmonics. However, small changes in circuit parameters can shift the resonance frequency, potentially introducing the risk of parallel resonance. This situation can cause harmonic expansion at unintended frequencies due to the interaction between the filter and the network impedance. Therefore, in the design of single-tuned harmonic filters, careful dimensioning is required to minimize both the attenuation effectiveness and the risk of parallel resonance [15, 16].

2.2. First-Order High-Pass Filter

First-order high-pass filters are among the simplest shunt filter topologies for harmonic suppression, featuring a series RC structure. The impedance of these filters in Laplace space is:

$$Z_f(s) = \frac{RCs + 1}{Cs} \tag{4}$$

A first-order high-pass filter acts as an attenuator by providing a low-impedance path to ground for harmonic components above its cutoff frequency. Therefore, it can be used to attenuate a wide range of harmonics. However, since there is no inductance in the circuit, the quality factor (Q) is undefined. The

most significant disadvantage of this topology is that it causes high losses due to its nearly pure resistive characteristic at the fundamental frequency. Furthermore, the need for capacitor banks with high MVAr values to effectively suppress a wide harmonic band increases design costs and dimensions [17, 18].

2.3. Second-Order High-Pass Filter

Second-order high-pass filters include a damping resistor (Rd) connected in series with a capacitor and an inductance element in addition to the classic high-pass filter topology. This structure significantly improves filter performance. The impedance expression in Laplace space is:

$$Z_f(s) = \frac{RLCs^2 + Ls + R}{s(CLs + CRd)} \tag{5}$$

The most important advantage of second-order high-pass filters is that they have a shallower notch than single-tuned harmonic filters. This feature enables the filter to suppress multiple high-order harmonic components simultaneously. Additionally, the presence of damping resistance reduces sensitivity to parameter deviations and makes the filter more stable against misalignment. Compared to a first-order high-pass filter, this filter operates with lower fundamental frequency losses and provides more reliable performance with inductive loads. Due to these superior characteristics, it is among the most widely used high-pass filter topologies, particularly in industrial applications such as high-power variable speed drives (VSDs) [19].

2.4. Third-Order High-Pass Filter

Third-order high-pass filters are an improved version of the second-order high-pass filter topology, with the impedance of the resistive branch at low frequencies increased by adding a second capacitor ($C2$). The general impedance expression of this structure in Laplace space is:

$$Z_f(s) = \frac{RLC_1Cs^3 + (C_1 + C_2)Ls^2 + C_2Rs + 1}{sC_1(C_2Ls^2 + C_2Rs + 1)} \tag{6}$$

Compared to second-order high-pass filters, these filters further reduce losses at the fundamental frequency and offer more effective results, particularly in suppressing low-order harmonics. However, they are not as efficient as second-order high-pass filters in eliminating high-order harmonics. Furthermore, the increased number of elements leads to greater circuit complexity and higher costs, which limits the practical application of third-order high-pass filters. These filters are preferred in specialized industrial applications where harmonic limits are extremely strict [20, 21].

2.5. C-Type Filter

C-type filters are a modified derivative of the second-order high-pass filter topology and were developed to reduce losses at the fundamental frequency. In this structure, an auxiliary capacitor (C_2) has been added in series with the inductance. The general impedance expression is given in equation (7) in Laplace space:

$$Z_f(s) = \frac{LRC_1C_2s^3 + LC_2s^2 + (C_1 + C_2)Rs + 1}{sC_1(LC_2s^2 + RC_2s + 1)} \tag{7}$$

The reactance of the auxiliary capacitor is adjusted to compensate for the reactance of the inductance at the fundamental frequency. This provides a low-impedance path for the fundamental component current preventing losses in the resistive branch. This feature enables low fundamental frequency losses, one of the most important advantages of C-type filters. C-type filters are widely used in industry because they offer high attenuation performance at the set frequency and are particularly effective at low-order harmonics. However, they are less effective than second-order high-pass filters at attenuating high-order harmonics. This topology, which exhibits intermediate behavior between second- and third-order high-pass filters due to its low loss characteristic, is preferred for suppressing low-frequency harmonics and

interharmonics originating from high-power industrial VSDs, arc furnaces, and high-voltage direct current (HVDC) transmission systems [22, 23].

3. OPTIMIZATION FRAMEWORK

In this study, four different metaheuristic algorithms listed below were used in the optimization process [24, 25].

Genetic Algorithm (GA): Inspired principles of by biological evolution, GA represents solution candidates as chromosomes. New individuals are produced through selection, crossover, and mutation mechanisms via the fitness function. The basic update equation can be expressed as follows:

$$P^{t+1} = Selection(Crossover(P^t), Mutation(P^t)) \tag{8}$$

Here, Pt represents the population in the tth generation. This population-based global search mechanism offers powerful exploration capabilities in nonlinear multi-objective problems.

Particle Swarm Optimization (PSO): Developed by Kennedy and Eberhart, PSO is inspired by the collective movements of flocks of birds and schools of fish. Candidate solutions are modeled as particles, and each particle updates its velocity and position using both its own best experience ($pbest$) and the swarm's global best knowledge ($gbest$) to update its velocity and position, as shown in equations 9 and 10.

$$P^{t+1} = Selection(Crossover(P^t), Mutation(P^t)) \tag{9}$$

$$x_i^{t+1} = x_i^t + v_i^{t+1} \tag{10}$$

Here, ω is the inertial mass, c1 and c2 are acceleration coefficients, and r1 and r2 are random numbers. Thanks to its parametric simplicity and fast convergence, it has a wide range of applications, from energy systems to machine learning.

Differential Evolution (DE): DE stands out for its simple structure and diversity preservation capability. It generates new solutions by leveraging differences among individuals selected from the current population. Its basic equations are:

$$v_i^t = x_{r_1}^t + F \cdot (x_{r_2}^t - x_{r_3}^t) \tag{11}$$

$$u_i^t = Crossover(v_i^t, x_i^t) \tag{12}$$

Here, F is the scaling factor; r1, r2, r3 are different indices randomly selected from the population. The selection mechanism transfers more suitable individuals to the next generation. The balance between diversity and rapid convergence makes DE highly effective for parametric optimization.

Grey Wolf Optimization (GWO): Developed by Mirjalili and colleagues, GWO mathematically models the social hierarchy and hunting behavior of grey wolves. The equations of the enclosure mechanism;

$$\vec{D} = \left| \vec{C} \cdot \vec{X}_p(t) - \vec{X}(t) \right| \tag{13}$$

$$\vec{X}(t+1) = \vec{X}_p(t) - \vec{A} \cdot \vec{D} \tag{14}$$

Here, Xp is the position of the prey, A=2a·r-a, C=2r, and a is a coefficient that decreases linearly from 2 to 0. Leadership roles (α, β, δ) guide the pack, while other wolves (ω) update their positions according to this guidance.

3.1. Algorithmic Hyperparameters and Reproducibility Settings

In this study, all hyperparameters and boundary processing strategies of the four meta-heuristic optimization algorithms used (Genetic Algorithm – GA, Particle Swarm Optimization – PSO, Differential Evolution – DE, and Grey Wolf Optimization – GWO) are presented in this section to ensure methodological transparency and reproducibility (Table 2). The multi-criteria objective function is given in Eq. (15), simultaneously minimizing harmonic suppression, IEEE-519 standard compliance, and reactive power constraint (Qmax = 40 kVAr). Therefore, only algorithm-based settings and experiment configurations are reported in the Table 2.

Table 2. Hyperparameter settings for GA, PSO, DE, and GWO algorithms

Algorithm	Population/Swarm	Iterations/Generations	Key Parameters	Seed	Boundary Handling
GA	40 (Population Size)	60 (Max Generations)	MATLAB default crossover / mutation	rng(1)	Clipping
PSO	50 (Swarm Size)	120 (Max Iterations)	Standard velocity and acceleration coefficients	rng(1)	Clipping
DE (rand/1/bin)	STF:108, others:60	200	F = 0.6, CR = 0.9	rng(1)	Clipping
GWO	30 (pack size N)	150	a: 2 → 0 (linear decrease), α–β–δ leadership	rng(1)	Clipping

These hyperparameters ensure that all algorithms operate under the same conditions and in a reproducible manner. All optimization processes were initiated with the same random seed (rng(1)), and boundary violations were prevented using the clipping method. This configuration ensures that comparative analyses are conducted fairly and that the results obtained are reproducible.

4. MATERIAL AND METHOD

The dataset used in this study was obtained from three-phase electrical measurements conducted at an industrial facility. The database comprises 60 columns and covers both basic electrical quantities and harmonic components. The fundamental measurements include active power (P1–P3, W), reactive power (Q1–Q3, VAR), and apparent power (S1–S3, VA) values for each phase; phase currents (I1rms–I3rms, A) and phase voltages (U1rms–U3rms, V); line voltages (U12, U23, U13, V) and neutral current (Ineutral, A). In addition, harmonic current components between the 3rd and 21st orders for each phase are recorded as percentages, and phase-based total harmonic distortion ratios (ITHD1–ITHD3, %) are calculated. The power factors (PF1–PF3) and displacement power factors (dPF1–dPF3) included in the data set, along with the total power factor (PFtot, dPFtot) values, have also been recorded. This rich data structure provides a strong foundation for evaluating passive harmonic filter topologies with both directly measured electrical parameters and derived power quality indicators. In this study, these data were transferred to the MATLAB environment as an N×60 matrix and used as input data for optimization algorithms. Additionally, it has been observed that low-order harmonic components (particularly the 3rd, 5th, and 7th harmonics) are dominant in industrial plant measurements, whereas the amplitudes of high-order harmonics above the 15th harmonic remain below approximately 2%. This situation indicates that the system has a typical industrial harmonic profile characterised primarily by low-order distortions. In this study, the objective function simultaneously considers harmonic suppression, standard compliance, and compensation safety; its mathematical definition is as follows:

$$J = THDI_{mean} + 10 \times Penalty + 10^{-6} \times \max(Q_C - Q_{max}, 0) \tag{15}$$

Here, while aiming to reduce THDI_mean harmonic distortion, the Penalty enforces compliance with the Ih/I1 limits in IEEE 519; if the reactive power constraint is QC≤40 kVAr, it ensures the industrial applicability of compensation. The workflow summarized in Figure 1 extends from data preprocessing and harmonic spectrum extraction to modeling grid and filter topologies and optimization steps using GA, PSO, DE, and GWO. Performance was evaluated based on THDI_mean, Penalty, and QC components; the obtained optimal L–C–R values were converted into engineering units and presented.

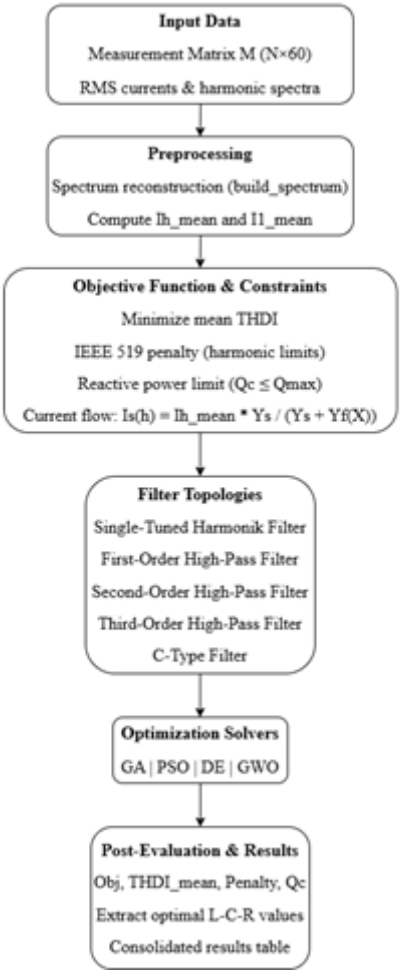

Figure 1. Workflow of the optimization framework

Table 3 summarizes the optimization outputs of four meta-heuristic solver combinations with five passive filter topologies. The results show that the single-tuned harmonic filter paired with the PSO and DE algorithms, yields the lowest objective function value (Obj ≈ 12.93) and the lowest average harmonic distortion (THDI_mean ≈ 0.577). This finding confirms the superior performance of this topology in suppressing low-order harmonics. In contrast, the first-order high-pass filter produced high Obj values (> 35) under all solvers and, due to its structural characteristics, was inadequate for low-order harmonics.

Table 3. Optimization results of filter topologies under different solvents

Topology	Solver	Obj	THDI_mean	Penalty	QC
Single-Tuned Harmonic Filter	solve_GA	13.45901283	0.594171159	1.284686683	57974.84335
	solve_PSO	12.93349143	0.577112819	1.233655012	59828.49031
	solve_DE	12.93349078	0.577112888	1.23365494	59828.4904
	solve_GWO	14.22041906	0.615360032	1.359321299	51846.03789
1st-Order High-Pass Filter	solve_GA	35.92041077	1.319917304	3.460049347	29804.76795
	solve_PSO	35.92040701	1.31991718	3.460048983	29914.24525
	solve_DE	35.92040701	1.31991718	3.460048983	29914.24525
	solve_GWO	35.92040701	1.31991718	3.460048983	29914.24525
2nd -Order High-Pass Filter	solve_GA	32.15300923	1.194106809	3.095890242	13064.38777
	solve_PSO	26.16370852	1.134009294	2.502969923	20058.66861
	solve_DE	25.62037126	1.034513439	2.458585782	27169.83617
	solve_GWO	25.27668091	1.025976424	2.425070449	29914.24525
3rd-Order High-Pass Filter	solve_GA	30.53551677	1.208159534	2.932735723	12928.84312
	solve_PSO	27.84287206	1.131275567	2.671159649	29914.24525
	solve_DE	27.84287167	1.131275576	2.671159609	29914.24525
	solve_GWO	27.85804871	1.131593202	2.67264555	29675.92992
C-Type Filter	solve_GA	28.26798371	1.108643308	2.715934041	12885.73558
	solve_PSO	26.85217211	1.067762241	2.578440986	19963.44161
	solve_DE	26.8521721	1.067762242	2.578440986	19963.44157
	solve_GWO	26.87362395	1.068477248	2.58051467	19971.61074

Figure 2 presents the Obj and THDI_mean values for different filter-solver combinations via bar graphs. The findings reveal that optimization performance cannot be evaluated based on a single criterion alone, but requires a multidimensional analysis. In particular, the single-tuned harmonic filter–PSO and single-tuned harmonic filter–DE combinations demonstrated clear superiority, providing the lowest Obj (~12.93) and THDI_mean (~0.577) values. In contrast, the first-order high-pass filter topology produced high Obj (>35) and THDI_mean (>1.3) values under all solvers, confirming its inadequacy in suppressing low-order harmonics.

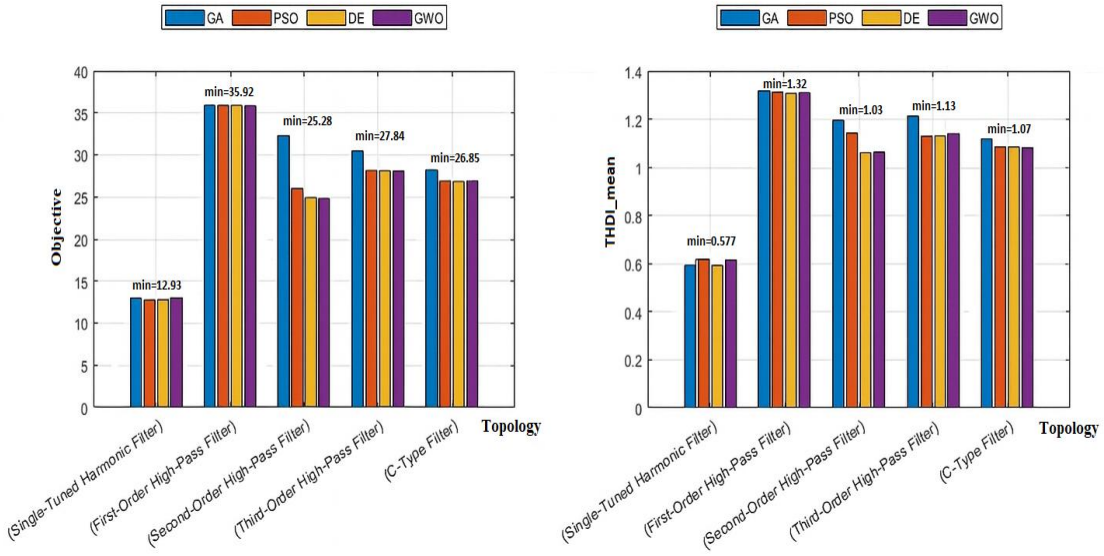

Figure 2. Comparison of Objective and THDI_mean values

Figure 3 compares solver–topology combinations using heat maps of normalized values for the Obj and THDI_mean metrics. The visual clearly demonstrates how harmonic suppression performance varies under different solvers. Specifically, the single-tuned harmonic filter–PSO and single-tuned harmonic filter–DE solutions stood out with the lowest Obj (~12.93) and THDI_mean (~0.577) values, indicating that low-order harmonics could be effectively suppressed. In contrast, the first-order high-pass filter topology produced high Obj (>35) and THDI_mean (>1.3) values under all solvers, thus proving insufficient for suppressing low-order harmonics.

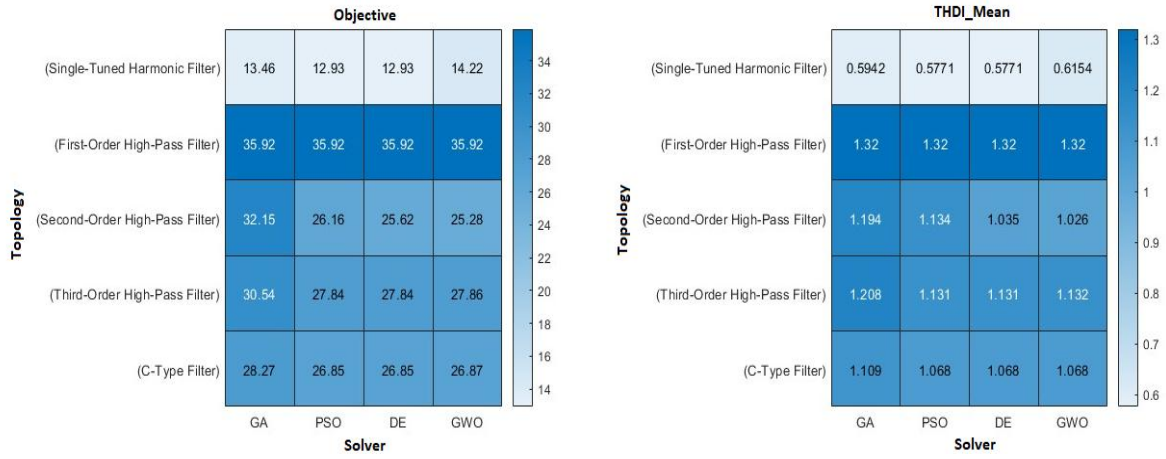

Figure 3. Comparison of the Objective and THDI_mean metrics

Figure 4 presents a comparative analysis of Penalty and QC results based on filter topologies and optimization solvers. In this analysis, the first-order high-pass filter topology produced consistent QC values (~2.9×10^4) across all solvers, but stood out with significantly high Penalty scores (>3.2). This confirms that the first-order high-pass filter fails to suppress low-order harmonics and is therefore an inadequate option under the IEEE-519 standard.

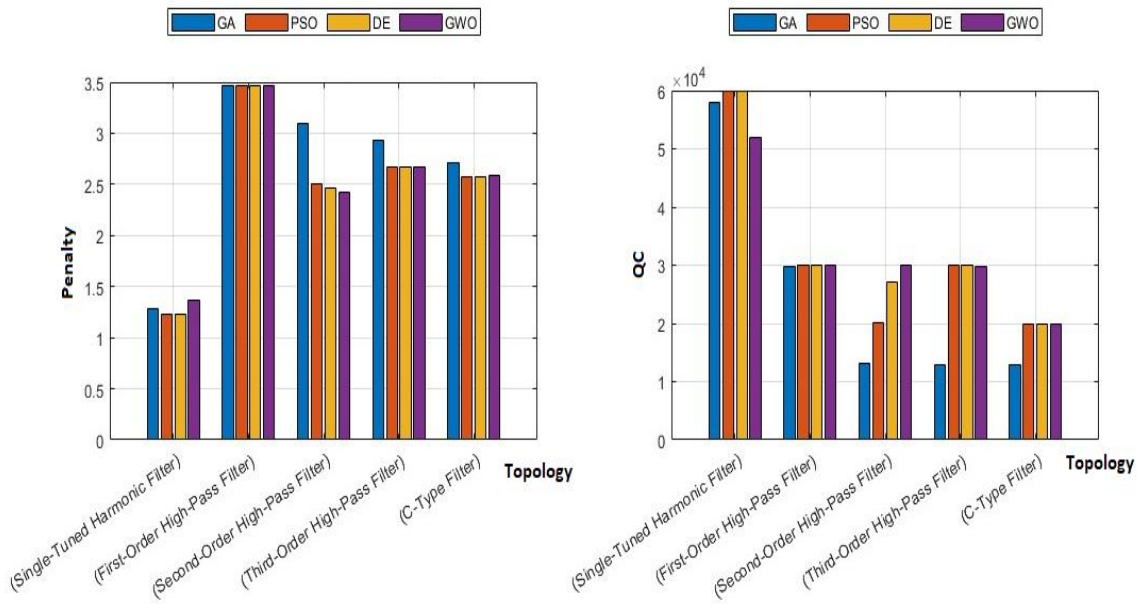

Figure 4. Comparison of Penalty and QC values for different filter–solvent combinations

The mutual interaction between the objective and QC is shown in Figure 5. The graph presents the position of each topology–solver combination in the two-dimensional performance space, while the Pareto curve represents only non-dominated solutions. This approach supports a multi-criteria decision-making process that simultaneously considers harmonic reduction (Obj minimization) and compensation stability (QC minimization). The findings reveal that single-tuned harmonic filters and C-type filter topologies are positioned on the Pareto front, representing the strategies closest to the optimal solution. Single-tuned harmonic filter solutions achieve strong harmonic suppression with very low Obj values (~12–14), but carry the risk of reactive power instability due to high QC (~5.5–6.0 × 10^4). In contrast, C-type filter–PSO/DE solutions, despite exhibiting relatively limited performance in harmonic reduction with medium Obj values (~26–28), offer an extremely balanced profile in terms of compensation stability thanks to low QC (~1.9 × 10^4). Second-order high-pass filters and third-order high-pass filter solutions, while approaching the Pareto front, could not be considered fully optimal options due to either high Objective or high QC values. In particular, the first-order high-pass filter topology showed the weakest performance in terms of both harmonic reduction and reactive power control with a combination of high Obj (>35) and medium QC (~2.9 × 10^4). These results confirm once again that optimization based on single metrics can be misleading; multi-criteria optimization is essential in real system designs. From the perspective of field applications, the balance provided by the C-type filter topology between reactive power compensation stability and harmonic compliance stands out as a sustainable solution for modern industrial systems.

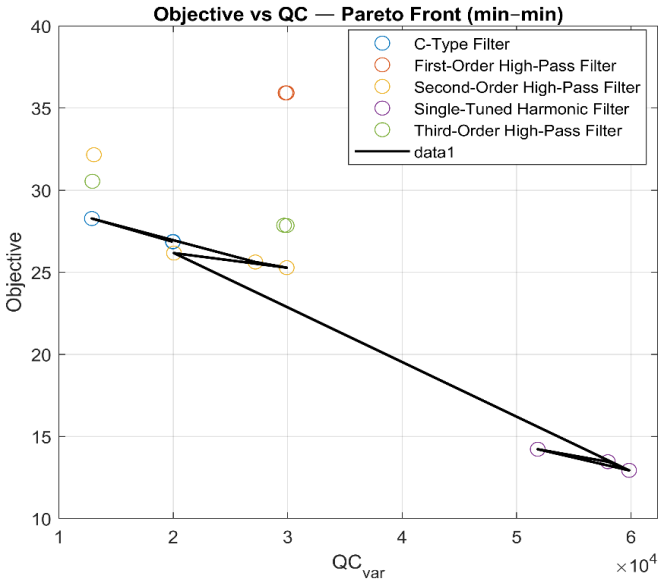

Figure 5. Pareto front analysis between Objective and QC

Figure 6 shows the Objective, THDI_mean, Penalty, and QC metrics on a normalized radar chart. This method supports decision-making by combining the multidimensional performance profiles of different solver–topology combinations in a single visual. The more compact radar area indicates that a balanced and sustainable solution is achieved across multiple performance criteria. The analysis findings reveal that the second-order high-pass filter–DE and C-type filter–PSO solutions produce compact radar areas with low Penalty (~2.58) and QC (~1.9 × 10^4) values, thereby achieving an optimal balance between harmonic suppression, standard compliance, and reactive power stability. In contrast, the first-order high-pass filter topology exhibited a wide radar area under all solvers, showing poor performance with high Obj (>35) and Penalty (>3.2) values. Single-tuned harmonic filter solutions, despite their low Objective (~13) advantage, created instability in the radar area due to high QC values (~5.5–6.0 × 10^4) and lagged behind in multidimensional optimization. As a result, it demonstrates that the combinations of C-type filter–PSO and second-order high-pass filter–DE are the most balanced and sustainable design alternatives that simultaneously consider harmonic suppression, compliance with standards, and reactive power stability.

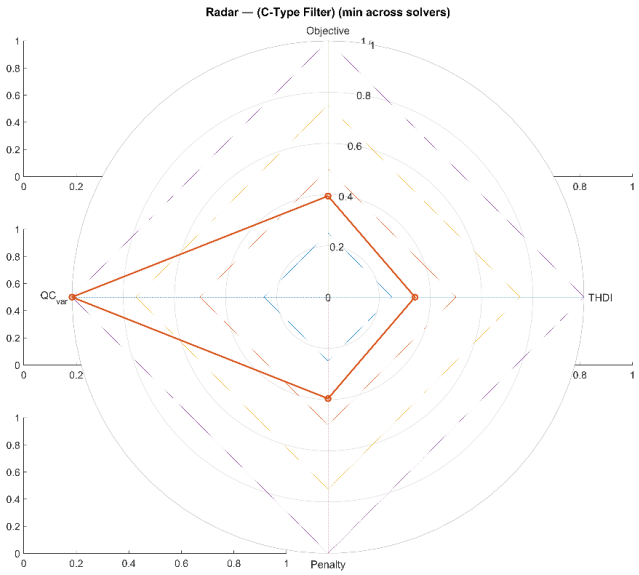

Figure 6. Radar chart of normalized performance metrics

The comparative parameter distributions of single-tuned harmonic filters at different harmonic orders are shown in Figure 7. The graphs show capacitor values, inductor, and resistance values, respectively, and the parameter sensitivity of the solution sets has been evaluated across harmonic orders. The analysis findings reveal that the single-tuned harmonic filter topology stands out with high capacitance (~380 μF), high inductance (~2.1 mH), and relatively high resistance (~0.041 Ω) values, especially in the h3 harmonic component; in contrast, these parameters decrease to lower values in the h7 harmonics. This indicates that the single-stage harmonic filter has higher sensitivity and damping capacity against lower-order harmonics, while exhibiting passive behavior at higher orders.

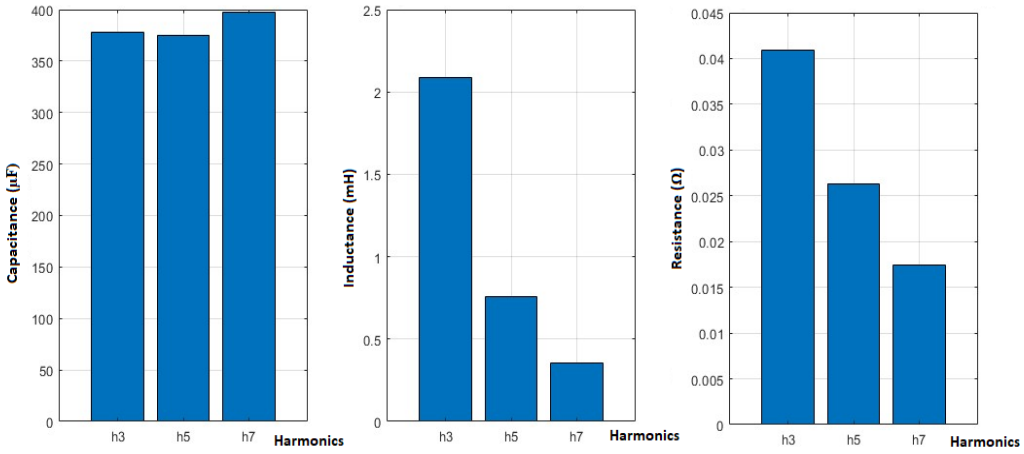

Figure 7. Distribution of optimal L–C–R parameters for a single-tuned harmonic filter.

5. COMPARATIVE ANALYSIS WITH PREVIOUS STUDIES

This study addresses passive harmonic filter (PHF) design within a multi-topology (STF, HPF-1/2/3, C-Type) and multi-algorithm (GA, PSO, DE, GWO) framework by simultaneously optimizing the THDI_mean, IEEE-519 penalty, and QC ≤ 40 kVAr objectives/constraints. Below is a positioning of the study in relative to frequently cited works in the literature in terms of methodological scope and the criteria evaluated.

Özer et al. [2], focus on the classification of power quality degradation; they reports 99.33% overall success in a multi-class scenario. Represents the upper limit on the monitoring/decision-support axis; PHF sizing/optimization is outside the scope. Chang & Wu [7], single-topology focused, with TDD_I/THD_V minimization prioritized. Under sample conditions, harmonic currents were 8.76, 5.78, 2.88, and 2.94%, and TDD_I reached 14.45%, indicating limit exceedances. The difference from our work is that multi-criteria (THDI_mean + IEEE-519 penalty + QC) and multi-topology comparisons are not performed together. Shaikh et al. [25], focus on convergence/time efficiency with the HGWPSO approach (the subject is not PHF, but transmission line parameter estimation). Average improvements in three tests were 0.15%, 4.85%, 2.84%; CPU times were reported as ~0.8986 s for HGWPSO, GWO: 1.5331 s, PSO: 1.9001 s. Methodologically, it is close to multi-criteria optimization; however, the application objective is different. Milovanović et al. [26], MOGA is used for location and parameter optimization in unbalanced systems. In one scenario, max. THD_V decreases by 77.76%, while max. VUF increases by 71.55%; the study examines trade-offs while observing IEEE-519 limits. Our approach optimizes different PHF topologies and solvers together on the same industrial dataset while observing QC security (IEEE-519 compliance). Yang & Le [27], multi-objective optimization logic is established in PPF design with MOBA + Pareto; a clear trade-off between cost–THD–reactive compensation is demonstrated. While this work strengthens the methodological foundation, our approach extends this logic to the multi-topology + multi-algorithm level. Contribution and Positioning. To overcome the limitations of past approaches focused on single-topology and/or single-criterion (THD only), we propose a multi-criteria template that compares multiple topologies and solvers under the same industrial conditions and equal terms. The reported values of THDI_mean ≈ 0.577, Penalty ≈ 2.58, and

QC ≈ 1.996×10⁴ VAr indicate that a balanced design point between standard compliance and reactive balance can be achieved.

6. RESULTS AND DISCUSSION

In this study, five passive harmonic filter topologies (single-tuned harmonic filter, high-pass filter, second-order high-pass filter, third-order high-pass filter, and C-type filter) were comprehensively optimized and compared using four advanced solvers (GA, PSO, DE, and GWO). The proposed framework not only examined harmonic reduction performance but also extended to include IEEE-519 compliance analysis, QC, multi-objective Pareto evaluation, radar-based holistic comparison, and robustness–sensitivity analysis. The main findings can be summarized as follows:

- Penalty function and QC analyses revealed that the first-order high-pass filter topology produced high penalty values (>3.2) and failed to meet the IEEE-519 standard. In contrast, C-type filters, particularly under PSO and DE optimization, yielded the lowest penalty value (~2.58) and balanced QC level (~19.963), demonstrating superior performance in standard compliance and reactive power stability.
- Pareto front analysis confirms that single-tuned harmonic filters and C-type filters are closer to the optimal solution and offer the most balanced performance between harmonic suppression and reactive power control. This clearly demonstrates the advantages of single-tuned harmonic filters and C-type filters when both must be optimized together in practical designs.
- Radar-based comprehensive evaluation has shown that second-order high-pass filters–DE and C-type–PSO solutions have compact, symmetric areas, thus offering balanced performance across multiple criteria. In contrast, the first-order high-pass filter exhibited a wide and unbalanced radar area, confirming its industrial inadequacy.
- Durability and sensitivity tests have demonstrated that single-tuned harmonic filters and C-type filters maintain stable performance even under variable harmonic conditions, whereas first-order high-pass filters experience significant fluctuations. In particular, single-tuned harmonic filter–PSO/DE combinations offered the most reliable solutions in terms of harmonic suppression performance and reactive power compensation.

In general, the findings indicate that C-type and single-stage harmonic filters demonstrate high efficiency and stable performance, particularly in industrial systems where low-order harmonics (h3–h7) are dominant. However, in systems where high-order harmonic components (>h15) are prominent, alternative filter topologies or active–passive hybrid structures may offer better performance. Furthermore, in industrial facilities with different harmonic spectra, such as those with inverter-based or variable-speed drive systems, the distribution and interaction of harmonics can vary significantly, potentially altering the relative effectiveness ranking of filter topologies. This situation highlights the need to generalise the proposed optimisation framework to multiple harmonic spectrum scenarios in future studies. C-type filters stand out for minimizing standard violations and maintaining reactive power balance, while single-stage harmonic filters are distinguished by their effective suppression of low-order harmonics and high durability. However, the structural limitations of the first-order high-pass filter topology restrict its practical applicability, particularly in power systems where low-order harmonics are dominant.

6.1. Algorithmic Hyperparameters and Reproducibility Settings

This study has comparatively evaluated the performance of passive harmonic filter (PHF) topologies using a multi-criteria optimization approach and has presented results with high industrial applicability. However, the scope of the proposed method is subject to certain limitations:

System Specificity: The optimization process is based on measurements from a specific industrial facility. Differences in impedance structure, load profiles, or harmonic components in different industrial facilities may limit its general applicability.

Simplified Network Model: Network Modeling Simplification: In the analytical evaluation, short-circuit power was assumed to be constant; load dynamics and frequency-dependent source/line impedance

effects were not included in the model. This simplification may partially limit field accuracy under different operating conditions.

Component Realism: Filter elements (L, C, R) have been optimized under the assumption of ideal electrical behavior. In real conditions, thermal effects, frequency deviations, and component aging may alter performance to some extent.

Lack of Experimental Validation: The analyses in this study were performed using numerical simulations. Future work plans to experimentally validate the proposed optimization framework on a physical test setup.

These limitations provide guidance for further development of the proposed method. Future research plans include applying the model to hybrid active–passive filter systems, multi-objective artificial intelligence-based optimizations, and real-time adaptive compensation systems. This will enable harmonic suppression, compliance with standards, and reactive power stability in industrial power systems, thereby achieving a more dynamic and scalable structure.

Conflict of Interest Statement

There is no conflict of interest between the authors.

Statement of Research and Publication Ethics

The study is complied with research and publication ethics.

Artificial Intelligence (AI) Contribution Statement

In this study, artificial intelligence (AI) tools were used for purpose of improving the grammatical accuracy and linguistic clarity of the text. All scientific content, including data analysis, figures, and the manuscript's structural composition, was entirely generated by the authors without any AI assistance.

Contributions of the Authors

A.N. and F.K. conceived the presented idea. F.K. developed the theory and performed the calculations. A.N. edited and finalized the paper. All authors discussed the results and contributed to the final paper.

REFERENCES

[1] M. A. S. Masoum and E. F. Fuchs, Power Quality *in Power Systems and Electrical Machines*, Elsevier, USA, 2015.

[2] İ. Özer, S. B. Efe, and H. Özbay, "CNN / Bi-LSTM-based deep learning algorithm for classification of power quality disturbances by using spectrogram images," *International Transactions on Electrical Energy Systems,* 13204, pp. 1–16, 2021.

[3] M. Grady, "Understanding power system harmonics," *Department of Electrical & Computer Engineering*, University of Texas at Austin, Apr. 2012.

[4] S. Rüstemli and M. S. Cengiz, "Active filter solutions in energy systems," *Turkish Journal of Electrical Engineering & Computer Sciences,* vol. 23, pp. 1587–1607, 2015.

[5] Ö. F. Keçecioğlu, M. Tekin, A. Gani, H. Açıkgöz, A. Gemci, and M. Şekkeli, "Bir güneş enerji santralinin elektrik şebekesindeki güç kalitesi parametrelerine etkisinin incelenmesi," *KSÜ Mühendislik Bilimleri Dergisi,* vol. 18, no. 2, 2015.

[6] E. F. Fuchs and M. A. S. Masoum, *Power Quality in Power Systems and Electrical Machines*, Elsevier Academic Press, 2008, ISBN: 978-0-12-369536-9.

[7] Y. P. Chang and C. J. Wu, "Optimal multiobjective planning of large-scale passive harmonic filters using hybrid differential evolution method considering parameter and loading uncertainty*," IEEE Transactions on Power Delivery,* vol. 20, no. 1, pp. 408–416, Jan. 2005.

[8] A. F. Zobaa, "The optimal passive filters to minimize voltage harmonic distortion at a load bus," *IEEE Transactions on Power Delivery,* vol. 20, no. 2, pt. 2, pp. 1592–1597, Apr. 2005.

[9] R. C. Dugan, M. F. McGranaghan, S. Santoso, and H. W. Beaty, *Electrical Power Systems Quality*, 2nd ed., McGraw-Hill, 2004.

[10] J. C. Das, "Passive filters—Potentialities and limitations," *IEEE Transactions on Industry Applications,* vol. 40, no. 1, pp. 232–241, Jan. 2004.

[11] M. Tekin and A. S. Yılmaz, "Güç sistem harmoniklerinin ayrık Hartley dönüşümü ile incelenmesi," *V. Enerji Verimliliği ve Kalitesi Sempozyumu Bildirileri,* 2013.

[12] American Bureau of Shipping, Guidance Notes on Control of Harmonics in Electrical Power Systems, *American Bureau of Shipping,* Spring, TX, USA, 2006.

[13] D. M. Soomro and M. M. Almelian, "Optimal design of a single tuned passive filter to mitigate harmonics in power frequency," *ARPN Journal of Engineering and Applied Sciences*, vol. 10, no. 19, pp. 9009–9014, 2015.

[14] A. Ahmed, A. Eman, E. Ragab, E. Adel, and F. Khaled, "Comprehensive parametric analysis of single tuned filter in distribution systems," *in Proc. 21st Int. Middle East Power Systems Conf.* (MEPCON), 2019, pp. 465–472.

[15] O. T. Tawfeeq, "THD reduction of a current source rectifier-DC motor drive using single tuned filters," *International Journal of Inventive Engineering and Sciences (IJIES),* vol. 1, no. 12, Nov. 2013.

[16] H. A. M. Ali, A. F. Zobaa, and E. E. A. El-Zahab, "Single-tuned passive harmonic filters design with uncertain source and load characteristics," *Recent Patents on Electrical Engineering*, vol. 5, no. 1, pp. 72–80, 2012.

[17] J.-W. Horng, C.-M. Wu, J.-H. Zheng, and S.-Y. Li, "Current-mode first-order high-pass, low-pass, and all-pass filters using two ICCIIs," *IEEE Int. Conf. on Consumer Electronics,* Taiwan (ICCE-Taiwan), 2020, pp. 1–2.

[18] D. Agrawal and S. Maheshwari, "An active-C current-mode universal first-order filter and oscillator," *Journal of Circuits, Systems and Computers*, vol. 28, 2019.

[19] Y. Patil, P. Naik, P. Shettar, S. Angadi, and S. Kotabagi, "Active filter design—Second order low pass and high pass," in Global Conf. on Communications and Information Technologies (GCCIT), Bangalore, India, 2024, pp. 1–8.

[20] H. A. A. Shady, F. Z. Ahmed, and E. B. Murat, "Optimal resonance-free third-order high-pass filters based on minimization of the total cost of the filters using Crow Search," *Electric Power Systems Research,* vol. 151, pp. 381–394, 2017.

[21] H. Tarunkumar, A. Ranjan, S. Perumalla, and N. M. Pheiroijam, "Four input single output based third order universal filter using four terminal floating nullor," *Analog Integrated Circuits and Signal Processing*, vol. 93, no. 1, pp. 87–98, Oct. 2017.

[22] K. Liu, F. Yang, Y. Wang, et al., "Analysis of the intrinsic characteristics of C-type damped filter and its optimal application scenario," *Electric Power,* vol. 56, no. 7, pp. 125–135, 2023.

[23] Y. Xiao, J. Zhao, and S. J. Mao, "Theory for the design of C-type filter," *in Proc. 11th Int. Conf. on Harmonics and Quality of Power (ICHQP),* Lake Placid, NY, USA, 2005, pp. 11–15.

[24] M. C. Aguitoni, L. V. Pavão, P. H. Siqueira, L. Jiménez, and M. A. S. S. Ravagnani, "Heat exchanger network synthesis using genetic algorithm and differential evolution," *Computers & Chemical Engineering,* vol. 117, pp. 82–96, 2018.

[25] M. S. Shaikh, H. Lin, G. Zheng, C. Wang, Y. Lin, and X. Dong, "Innovative hybrid grey wolf-particle swarm optimization for calculating transmission line parameter," *Heliyon,* vol. 10, no. 10, e38555, 2024.

[26] M. J. Milovanovic, S. S. Raicevic, D. Klimenta, N. Raicevic, and B. D. Perovic, "Determination of optimal locations and parameters of passive harmonic filters in unbalanced systems using the multiobjective genetic algorithm," *Elektronika ir Elektrotechnika,* vol. 30, no. 12, 2024.

[27] N.-C. Yang and M.-D. Le, "Optimal design of passive power filters based on multi-objective bat algorithm and Pareto front," *Applied Soft Computing*, vol. 35, pp. 257–266, 2015.